*32nd EPS Conference on Plasma Phys. Tarragona, 27 June - 1 July 2005 ECA Vol.**29C**, P-5.029 (2005)*

Effect of suprathermal electrons on impurity ionization state

M. A. Ochando, F. Medina, B. Zurro, K. J. McCarthy, J. A. Jiménez, A. Baciero, D. Rapisarda, J. M. Carmona and D. Jiménez

Laboratorio Nacional de Fusión. Asociación EURATOM/CIEMAT, 28040 Madrid, Spain

Introduction

Impurity behavior as a function of magnetic topology is an important object of study in TJ-II. Some robust structures in chord-integrated radiation profiles of the 227.1 nm line emission of CV were detected in radial positions where the rotational transform has a rational value [1]. In impurity injection experiments using the laser blow-off technique, it was found that the relaxation of the global emission perturbation caused by the non-intrinsic impurity ions could not be fitted by a pure exponential function [2]. These studies were done with spatial resolution using broadband, bolometer, and soft x-ray detector arrays located in different toroidal positions. The adjusting parameters necessary to describe the intensity decay varied with the magnetic configuration and, in any case, they showed a non-monotonic dependence on plasma minor radius.

In parallel with tracking of injected impurities, the behavior of suprathermal electrons in plasmas with different magnetic configurations and electron densities is being also investigated in TJ-II. Some previous experimental findings related to this are: i) rational surfaces are good confinement regions for high-energy electrons, that is, the radial transport of such electrons cannot be expressed as smooth functions of the minor radius [3] and ii) there are toroidally asymmetric fluxes of ripple-trapped suprathermal electrons that can be modified by the presence of relevant (low order) rational surfaces [4].

In the present work, we give an explanation compatible with the unexpected temporal response of plasma emissivity to iron injection observed in experiments recently performed in TJ-II.

Experimental

For this experiment, TJ-II plasmas were produced and maintained with electron cyclotron resonance heating (ECRH) (2 x 300 kW gyrotrons, at 53.2 GHz, 2nd harmonic, X-mode polarization). Iron tracer ions were injected into almost stationary phases of ECRH plasmas using the laser ablation technique. Thin films of material deposited onto the surface of a glass substrate were ablated by short pulses produced by a focused Q-switched Nd-YAG laser beam (800 mJ, 10 ns).

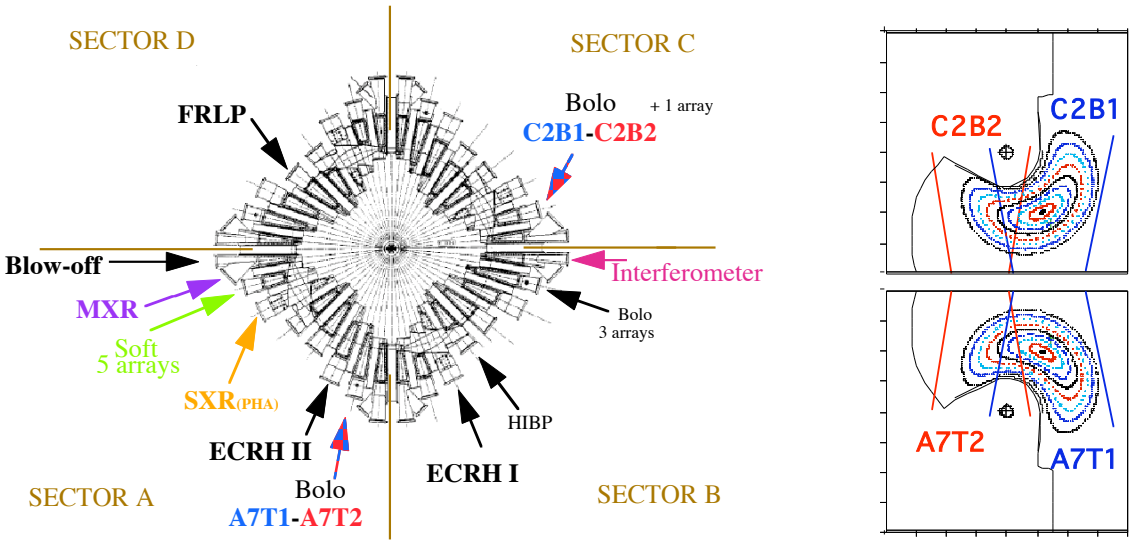

Figure 1. left) TJ-II diagnostics set-up. right) plasma cross section in equivalent sectors and twin-bolometers viewing volumes.

The laser ablation system of TJ-II is described in more detail in ref. [2]. The standard system of detectors used in impurity transport studies are x-ray monitors with different energy windows (80-200 keV- HXR; 20-150 keV- MXR; 2-15 SXR and 0.8-5 keV/1.5-5 keV x-ray arrays), bolometer arrays and wide-angle bolometers (2eV-5 keV), an f/10.4 1m normal-incidence vacuum spectrometer (20-300 nm), and phosphor detectors sensitized to the VUV. Figure 1 left shows the toroidal locations of these systems as well as the position of the blow-off and ECRH injection ports. It must be noted here that TJ-II is a four period Heliac with 8 modules per period, designed in such a way that the modules n and 8-n+1 are mirror images with respect to the equatorial plane, or in other words, plasma cross sections at toroidal angles θº and (90-θ)º have up-down symmetry. Then, each pair of detectors labeled A7T1 and C2B1 and A7T2 and C2B2 (used as global radiation monitors) view equivalent plasma regions (see in Fig. 1 right the Poincaré plots at θ=75.5º and θ=15.5º for the magnetic configuration used in this experiment, with iota (0.75a)=8/5).

In Fig. 2 we have plotted the relevant signals for shot #11325, in which iron was injected at t=1116.2 ms. Radiation signal labels correspond to the detector names given in Fig. 1 left. The average electron density, the central ECE channel, the integrated flux of low (SXR), intermediate (MXR) and high-energy x-ray photons (HXR) and the injection monitor signal (LP) are also shown. Looking at the temporal evolution of the different radiation detectors immediately after the injection, one can see some unexpected behaviors. As above mentioned the signal HXR is the integrated flux of photons with energies higher than 80 keV that are generated when fast electrons collide with a massive bumper, e.g. limiters, probe tips, etc., or when they finally reach the vacuum vessel wall.

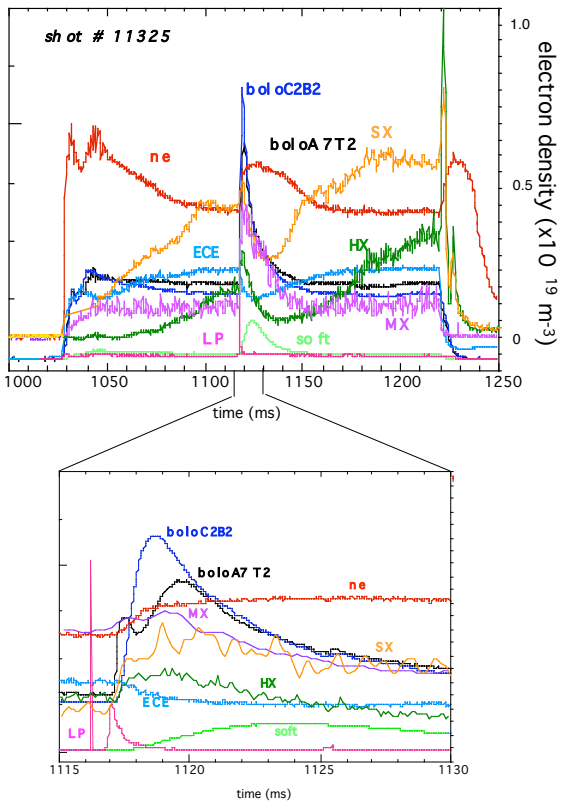

Figure 2. Temporal evolution of representative signals.

The production of such energetic electrons depends on the absorbed input power density [5], so that for a fixed heating power, as is the case here, the increase in electron density should be accompanied by a decrease in HXR, MXR and SXR signals. On the contrary, and despite the poor-time resolution of those signals, it can be seen how in the first step they increase as electron density does while the reaction time of signals from the central chords of the soft x ray cameras (0.8-5 keV energy range) located in the same toroidal region is longer than 1 ms. The change in the low-energy photon spectrum produced after the iron injection can be seen in Fig. 3: the iron Kα-line clearly appears and the intensity of

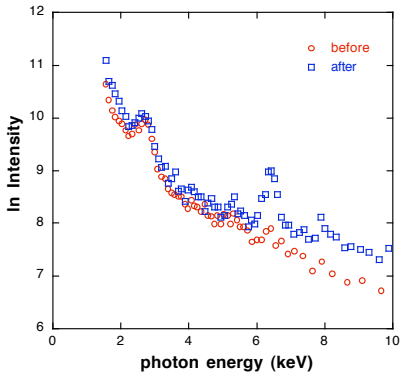

Figure 3. SXR spectra, before and after the iron injection

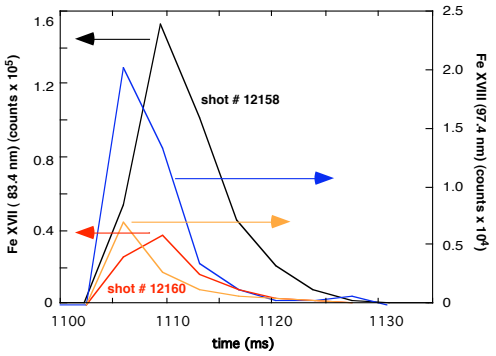

Figure 4. Line emissions of Fe XVII and Fe XVIII right after injection.

higher energy photons increases. The VUV spectrometer detects emission lines from highly ionized states of iron (Fe XVII and Fe XVIII) only right after the injection. All these observations indicate that the incoming iron is highly ionized (over-ionized) near the periphery due to collisions with high-energy electrons, either suprathermal trapped in the magnetic field ripple or fast passing linked to the 8/5 rational surface. That would give rise to anomalous increases of electron density and ion charge at specific radial positions.

At the same time, some of the bolometry signals exhibit unexpected behavior as well. When comparing the temporal evolution of signal A7T2 with that of its twin C2B2 (the same stands

for A7T1 and C2B1) it can be seen that near the gyrotron region the iron perturbation is detected before. Then signal A7T2 decreases before rising again while C2B2 signal shows the standard radiation response to an impurity injection pulse. To understand this behavior we have to recall the experimental finding of TJ-II that near the power injection port there is a strong convective flux of ripple-trapped suprathermal electrons [4]. The deformation of the electron distribution function, mainly due to the perpendicular resonant absorption of the microwaves, combined with the high helical ripple in TJ-II seems to confer to that region singular characteristics from the point of view of *effective* plasma parameters. The anomalous reduction of radiation is compatible with a decrease of the radiation strength of iron, due to a local (toroidal and/or radial) increase of electron "temperature". This hypothesis is verified with the injection represented in Fig. 4. There, the response of radiation signals to an injection of iron in a cold plasma is displayed. It can be seen that only bolometers in sector A7 detect the enhanced emission. This means that in this region there exist electrons with higher energy than in the rest of the device, that is, suprathermal electrons. And their energy is sufficient not only to produce excitations of the iron atoms but also ionizations, as the substantial increase of electron density confirms (also shown in Fig.4).

As the 'suprathermal effect' seems to be a rather universal phenomenon, this circumstance should be considered when impurity transport coefficients are evaluated in the frame of diffusive/convective models (*i.e.*, the inward convective velocity is proportional to the charge state of the impurity [6]), and when the time dependent diffusion coefficient is investigated in turbulent plasmas (*i.e.*, the Larmor radius has a strong effect on impurity ion transport [7]).

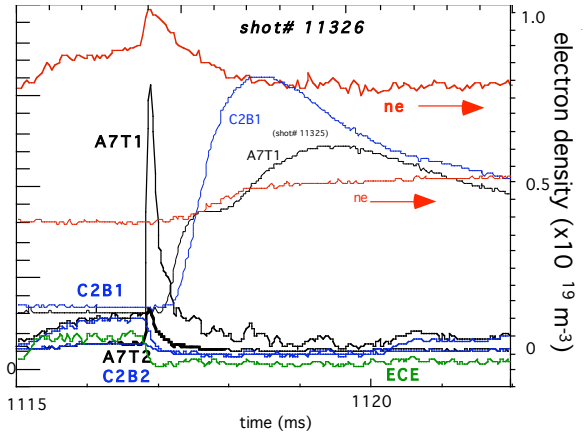

Figure 4. Iron injection in a cold plasma. Signals from the same shot of Fig. 2 are shown for comparison)

References

[1] A. Baciero et al., Plasma Phys. Controll. Fusion **43**, 1039 (2001).
[2] B. Zurro et al., 29th EPS Conf. Plasma Phys. Controll. Fusion, Vol. 26B P-5.025 Montreux ,2002.
[3] M. A. Ochando et al., 12th IAEA Stellarator Workshop, P2-19, Madison, 1999.
[4] M. A. Ochando and F. Medina, Plasma Phys. Controll. Fusion 45, 221 (2003)
[5] L. Rodríguez et al., 26th EPS Conf. Plasma Phys. Controll. Fusion, Vol. 23J, 353 (1999).
[6] H. Nozato et al., Phys. Plasmas 11,1920 (2004)
[7] M. Vlad et al., Plasma Phys Control. Fusion 47, 281 (2005)